Measurements on Higgs boson width and anomalous couplings with on-shell and off-shell production in ZZ decay channel at CMS experiment

Hanwen Wang

on behalf of the CMS collaboration
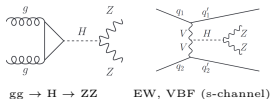
Beihang University &
Université Libre de Bruxelles

TeVPA 2021
October 27, 2021

Table of contents

- In SM H → VV decay mode, due to the fact that $m_V < m_H < 2m_V$, +10% of the events are produced through off-shell production mode in the region with $m_H^* \geq 2m_V$. The dominant processes are ggH and EW processes.

gg → H → ZZ   EW, VBF (s-channel)

- Due to unitarity, there is a large and negative Signal-Background interference in the SM in the offshell region.
  One of the goals of off-shell Higgs analysis is to test that there is a non-zero, negative and large interference between signal and continuum VV production mode.

- Presence of Higgs off-shell production can be quantified by measuring the signal strength parameters ($\mu = \sigma^{obs}/\sigma^{SM}$) such as $\mu_F^{off\text{-}shell}$ for ggH and $\mu_V^{off\text{-}shell}$ for EW, or a common $\mu^{off\text{-}shell}$ width different conditions on $R_{V,F}^{off\text{-}shell} = \mu_V^{off\text{-}shell}/\mu_F^{off\text{-}shell}$ to be = 1 or unconstraint.
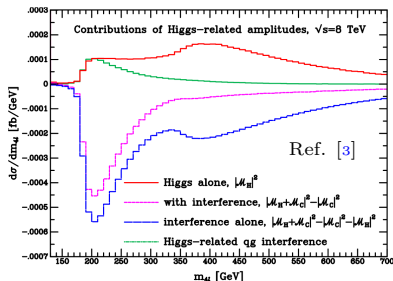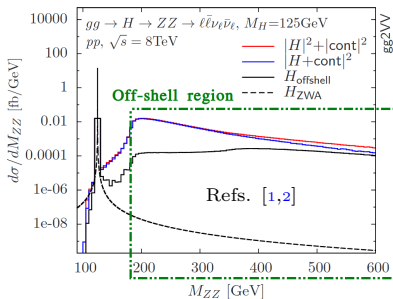
As pointed out in ref. [4] for a process such as $i \to H \to f$, the differential cross section is:

$$\frac{d\sigma_{i \to H \to f}}{dM_f^2} \sim \frac{g_i^2 g_f^2}{\left(M_f^2 - m_H^2\right)^2 + m_H^2 \Gamma_H^2} \qquad (1)$$

we can approximate the on-shell and off-shell cross sections such that,

$$\frac{\sigma^{\text{off-shell}}}{\sigma^{\text{on-shell}}} \propto \Gamma_H \qquad (2)$$

Therefore, off-shell results can be also interpreted in terms of Higgs total decay width Γ_H, if we combine $2\ell 2\nu$ off-shell and 4ℓ on-shell results.

Anomalous couplings of HVV interactions may also change the line-shape of m_{VV} and other kinematic variables.

These anomalous couplings can be parametrized through HVV amplitude as in ref.[5,6,7],

$$A_{(\text{HVV})} \sim \left[a_1^{\text{VV}} - e^{i\Phi_{\Lambda_1}} \frac{q_1^2 + q_2^2}{\Lambda_1^2} + \ldots \right] m_{\text{V}}^2 \epsilon_{\text{V1}}^* \epsilon_{\text{V2}}^* \qquad (3)$$
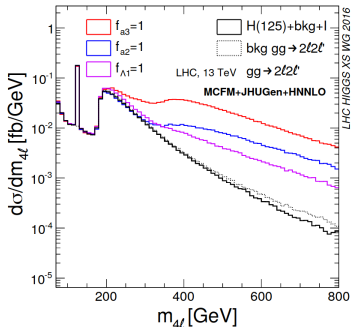
$$+ |a_2| e^{i\Phi_{a_2}} f_{\mu\nu}^{*(1)} f^{*(2),\mu\nu} + |a_3| e^{i\Phi_{a_3}} f_{\mu\nu}^{*(1)} \tilde{f}^{*(2),\mu\nu}$$

where in SM, $a_1 = 2$ and the rest 0.

In this analysis, we consider the extreme scenarios of anomalous couplings a_2, a_3, Λ_1, to constrain their strengh $\bar{f}_{ai} = f_{ai} \cos(\Phi_{ai})$ assuming $a_i \geq 0, \cos(\Phi_{ai}) = \pm 1$ where,

$$f_{ai} = \frac{|a_i|^2 \sigma_i}{\sum_j |a_j|^2 \sigma_j}, \ \ a_j = a_1, a_2, a_3, \frac{1}{\Lambda_1^2} \qquad (4)$$

$2\ell2\nu$ offshell data provide additional sensitivity to the $\bar{f}_{ai}$, and can be combined with the constraints from the 4ℓ onshell data.

- In this analysis we study the off-shell Higgs production in H → ZZ → 2ℓ2ν signal channel where $\ell = e, \mu$. The analysis is based on Data collected by CMS experiment during LHC run 2 (2016-2018) at $\sqrt{s} = 13$ TeV and with integrated luminosity of $\sim 138 \text{fb}^{-1}$.

- Signal and interfering backgrounds are modeled through matrix element reweighting techniques on POWHEG/JHUGen samples simulated at different Higgs pole mass.

- Results from off-shell $2\ell2\nu$ channel are combined with 4ℓ off-shell analysis from [8] to have meaningfull measurements on signal strength parameters (integrated luminosity $\leq 138 \text{fb}^{-1}$).

- For interpreting the results in terms of Γ_H and constraining anomalous couplings strength $(\bar{f}_{ai})$, the results from this analysis ($2\ell2\nu$ final state) are combined with 4ℓ on-shell analyses (integrated luminosity $\leq 140 \text{fb}^{-1}$) from [9,10].

Analysis PAS: HIG-21-013

Event selection and categorization

Events are categorized into $N_j = 0$, $N_j = 1$, $N_j \geq 2$, $\mu\mu$ and ee.

Event selections ("miss" $= p_{\mathrm{T}}^{\mathrm{miss}}$, j $=$ jet and $\ell = e, \mu$):

Quantity	Requirement
p_{T}^{ℓ}	$p_{\mathrm{T}}^{\ell} \geq 25\,\mathrm{GeV}$ on both leptons
$|\eta_\ell|$	< 2.4 on μ, < 2.5 on e
$m_{\ell\ell}$	$|m_{\ell\ell} - 91.2| < 15\,\mathrm{GeV}$
$p_{\mathrm{T}}^{\ell\ell}$	$\geq 55\,\mathrm{GeV}$
N_ℓ	Exactly two leptons with tight isolation, no extra leptons with loose isolation and $p_{\mathrm{T}} \geq 5\,\mathrm{GeV}$
N_{trk}	No isolated tracks satisfying the selection requirements
N_γ	No photons with $p_{\mathrm{T}} \geq 20\,\mathrm{GeV}$, $|\eta| < 2.5$ satisfying the baseline selection requirements
p_{T}^{j}	$\geq 30\,\mathrm{GeV}$, used in selecting jets
$|\eta_j|$	< 4.7, used in selecting jets
N_b	No b-tagged jets based on the loose working point
$p_{\mathrm{T}}^{\mathrm{miss}}$	$\geq 125\,\mathrm{GeV}$ if $N_j < 2$, $\geq 140\,\mathrm{GeV}$ otherwise
$\Delta\phi_{\mathrm{miss}}^{\ell\ell}$	> 1.0 between $\vec{p}_{\mathrm{T}}^{\ell\ell}$ and $\vec{p}_{\mathrm{T}}^{\mathrm{miss}}$
$\Delta\phi_{\mathrm{miss}}^{\ell\ell+\mathrm{jets}}$	> 2.5 between $(\vec{p}_{\mathrm{T}}^{\ell\ell} + \vec{p}_{\mathrm{T}}^{\mathrm{jets}})$ and $\vec{p}_{\mathrm{T}}^{\mathrm{miss}}$
min $\Delta\phi_{\mathrm{miss}}^{j}$	> 0.25 if $N_j = 1$, > 0.5 otherwise among all $\vec{p}_{\mathrm{T}}^{j}$ and $\vec{p}_{\mathrm{T}}^{\mathrm{miss}}$ combinations

- Due to the $2\ell2\nu$ final state in this analyis, the invariant mass of the ZZ system (m_{ZZ}) is not available, therefore it relies on characterizing an observable sensitive to m_{ZZ} that is the ZZ transverse mass m_T^{ZZ} defined as,

$$m_T^{ZZ\,2} = \left(\sqrt{p_T^{\ell\ell\,2} + m_{\ell\ell}^2} + \sqrt{p_T^{miss\,2} + m_Z^2} \, \right)^2 - \left(\vec{p}_T^{\,\ell\ell} + \vec{p}_T^{\,miss} \right)^2 \qquad (5)$$

- Different backgrounds behave differently along p_T^{miss}. The shape of this variable is also sensitive to the presence of SM or BSM Higgs signal. Thus, we explicitly use this observable in the measurements.

- In $N_j \geq 2$, matrix element discriminant ($\mathcal{D}_{2jet}^{VBF, a_i}$) can discriminate VBF production mechanism from ggH:

$$\mathcal{D}_{2jet}^{VBF, a_i} = \frac{\mathcal{P}_{VBF}^{a_i}}{\mathcal{P}_{VBF}^{a_i} + \mathcal{P}_{QCD\ H+2jet}^{SM}} \qquad (6)$$

where $\mathcal{P}$ is the matrix element probability density computed by MELA package [11] using kinematics from the two leading-p_T jets and the Higgs boson using $\eta_{\nu\nu} = \eta_{\ell\ell}$ approximation.

$\mathcal{D}_{2jet}^{VBF} = \mathcal{D}_{2jet}^{VBF, a_1}$ is always used and in SM-like analysis for the second discriminant, we use the one for $a_i = a_2$

- $qq \rightarrow \text{ZZ}$, WZ, the dominant backgrounds at high m_T^{ZZ}
  - Estimated from simulation
  - Joint fit with 3ℓ WZ control region (CR) to improve the estimation.

- Instrumental p_T^{miss} contamination from tails of p_T^{miss} in Drell-Yan process
  - Can not be well estimated from simulation
  - Estimated from single-photon CR(data-driven)
  - Real p_T^{miss} processes in this CR are estimated and subtracted from the reweighted data

- Nonresonant backgrounds (NRB)
  - Estimation from simulation is not optimal in our phase space
  - Estimated from $e\mu$ CR (data-driven)
  - Events are reweighted by lepton ID/isolation and trigger efficiencies,

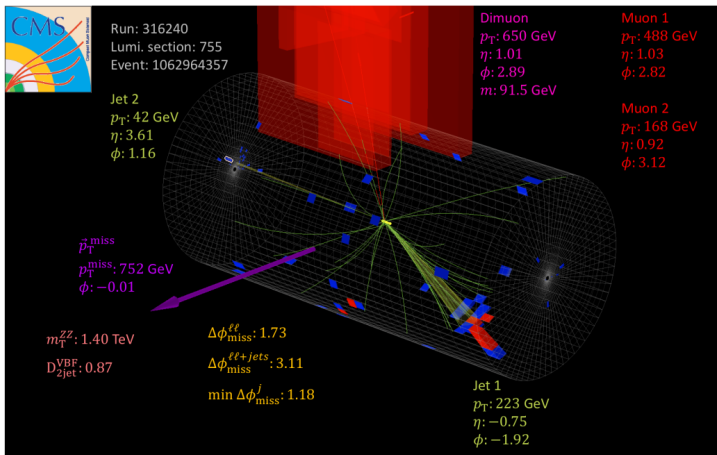- Minor contributions from e.g. $t\text{Z} + \text{X}$ processes are fully estimated from simulation

Figure 1 : Shown is a VBF/VBS candidate from the $N_j \geq 2$ category in the $2\ell2\nu$ signal region. The two jets pointed at opposite hemispheres, the high p_T^{miss} value, and the central, high-p_T dilepton system make this event one of the ideal candidates for this topology, as also evident by the high $\mathcal{D}_{2jet}^{VBF} = 0.87$ value computed for this event.
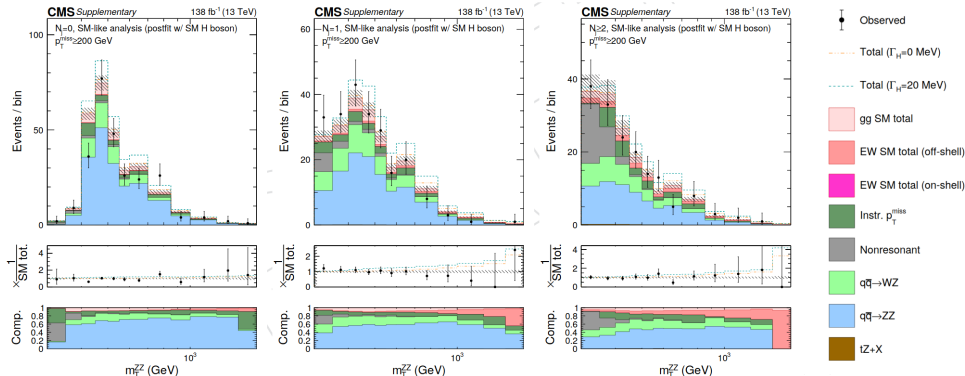
$m_\mathrm{T}^{\mathrm{ZZ}}$ distributions

Figure 2: Shows the postfit distributions of $m_\mathrm{T}^{\mathrm{ZZ}}$ in the $N_j = 0$ (left), $= 1$ (middle), and ≥ 2 (right) categories $2\ell2\nu$ signal region. Postfit refers to a combined $2\ell2\nu + 4\ell$ fit assuming SM H boson parameters. The middle pads on the bottom panels show the ratio of the data or dashed histograms to the stacked histogram, and the bottom pads show the relative contributions of each process in the stacked histogram
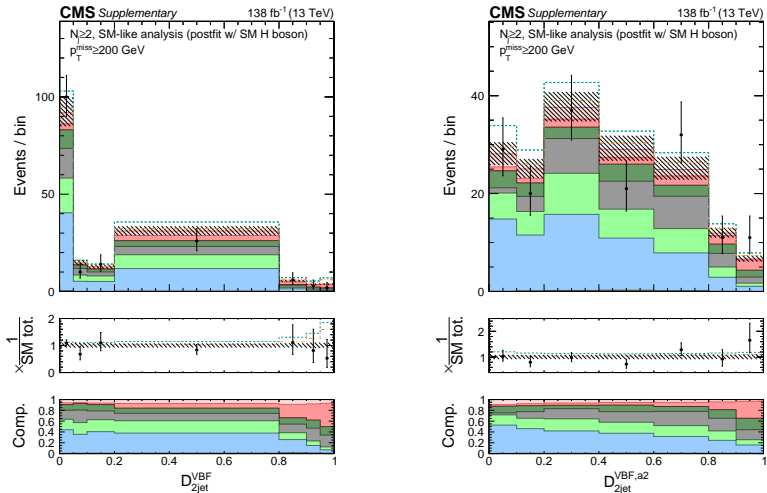
VBF kinematic discriminant distributions

Figure 2: Shows the postfit distributions of $\mathcal{D}_{2\mathrm{jet}}^{\mathrm{VBF}}$ (left) $\mathcal{D}_{2\mathrm{jet}}^{\mathrm{VBF},a2}$ (right) in the $N_j \geq 2$ category of $2\ell 2\nu$ signal region with an $p_{\mathrm{T}}^{\mathrm{miss}} \geq 200$ GeV requirement to enrich H boson contributions. Postfit refers to a combined $2\ell 2\nu + 4\ell$ fit assuming SM H boson parameters. The middle pads show the ratio of the data or dashed histograms to the stacked histogram, and the bottom pads show the relative contributions of each process in the stacked histogram.

Results on off-shell signal strength parameters
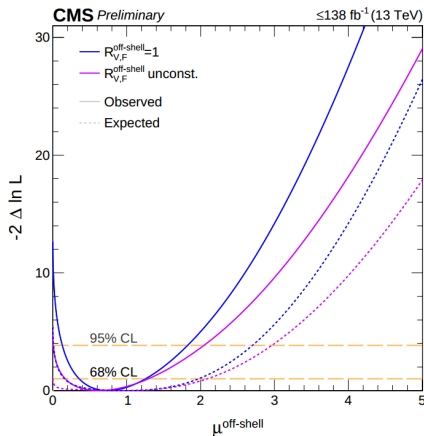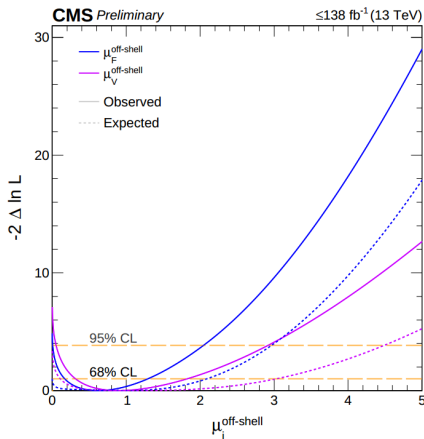
The scenario with $\mu^{\text{off-shell}} = 0$ ($R^{\text{off-shell}}_{\text{V,F}} = 1$) is excluded with more than 99.9% confidence (3.6 standard deviations).

Assuming no condition on $\mu^{\text{off-shell}}_{\text{V}}$, $\mu^{\text{off-shell}}_{\text{F}}$ is constrained at 95% confidence to be within the interval [0.0060, 2.0] and < 3.0 for observed and expected respectively.

Assuming no condition on $\mu^{\text{off-shell}}_{\text{F}}$, $\mu^{\text{off-shell}}_{\text{V}}$ is constrained at 95% confidence to be within the interval [0.051, 2.9] and < 4.5 for observed and expected respectively.

Results on off-shell signal strength parameters
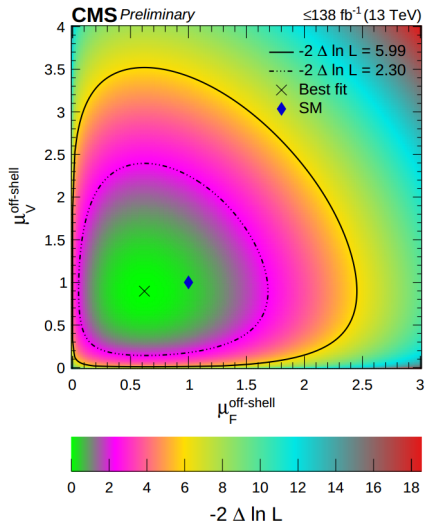
Figure 4: Shows the two-parameter likelihood scan of $\mu_{\mathrm{F}}^{\mathrm{off\text{-}shell}}$ and $\mu_{\mathrm{V}}^{\mathrm{off\text{-}shell}}$. The dot-dashed and solid contours enclose the 68% and 95% CL regions. The cross marks the minimum, and the blue rhombus mark is the SM expectation

Results interpretations on Higgs total decay width
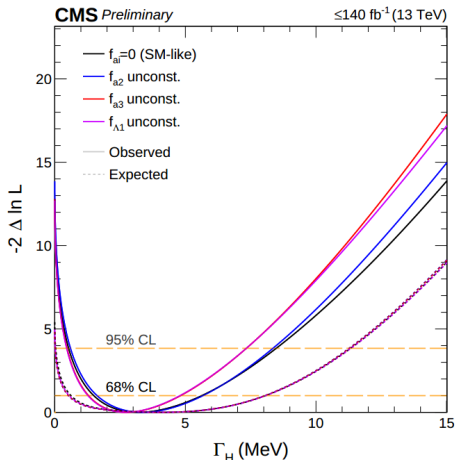

Figure 5: The likelihood scan of Γ_H with different constraints on Γ_H are shown with and without anomalous HVV couplings. The horizontal lines indicate the 68% and 95% CL regions.

The width of the H boson is observed to be $\Gamma_H = 3.2$ MeV and is constrained within the interval [0.53, 8.5] and [0.035, 11.3] at 95% confidence for observed and expected respectively.

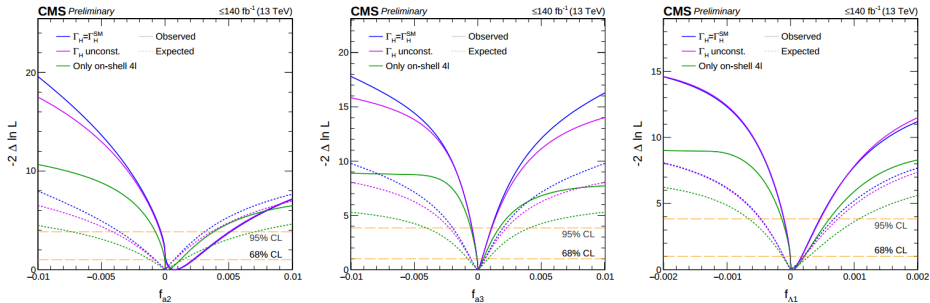# Results interpretations on BSM HVV couplings

Figure 6: Shows the likelihood scans of f_{a2} (left), f_{a3} (middle), and f_{Λ_1} (right) are shown with the constraint $\Gamma_H = \Gamma_H^{SM}$ (blue), Γ_H unconstrained (violet), or based on on-shell 4ℓ only (green). Observed (expected) scans are shown with solid (dashed) curves. The horizontal lines indicate the 68% and 95% CL regions.

- The CMS 2l2nu offshell analysis of 2016-2018 proton-proton collision data at 13 TeV c.m. energy was completed and shows good sensitivity to offshell ($m_{VV} > 2m_V$) H production.

- The combination of $2\ell2\nu$ off-shell analysis with published 4ℓ analyses [8,9,10] resulted in finding an evidence for the first time for off-shell Higgs production and the first time that Γ_H is measured ($\Gamma_H = 3.2$ MeV) with meaningful precision based on this evidence.

Backup

Table 2: Comparisons between the number of observed events in the $2\ell2\nu$ channel with expectations from the SM and no–off-shell scenarios as a function of N_j for low and high m_T^{ZZ}. An additional requirement of $p_T^{miss} \geq 200\,\text{GeV}$ has been imposed for $N_j \geq 2$.

	m_T^{ZZ}	$N_j = 0$	$Nj = 1$	$N_j \geq 2$
SM	$< 450\,\text{GeV}$	1118^{+45}_{-49}	660^{+31}_{-40}	92^{+7}_{-8}
No off.	$< 450\,\text{GeV}$	1127^{+46}_{-49}	666^{+31}_{-40}	93^{+7}_{-8}
Data	$< 450\,\text{GeV}$	989	643	95
SM	$\geq 450\,\text{GeV}$	241^{+13}_{-14}	166^{+10}_{-12}	68^{+5}_{-6}
No off.	$\geq 450\,\text{GeV}$	252^{+14}_{-14}	178^{+10}_{-13}	75^{+5}_{-6}
Data	$\geq 450\,\text{GeV}$	217	151	66

Table 4: Constraints on the $\mu_F^{\text{off-shell}}$, $\mu_V^{\text{off-shell}}$, and $\mu^{\text{off-shell}}$ parameters are summarized. The constraints on $\mu^{\text{off-shell}}$ are obtained with $R_{V,F}^{\text{off-shell}}$ unconstrained or $= 1$. The measurements are presented using the $2\ell2\nu$ analysis alone, or with the inclusion of off-shell 4ℓ events. The designation 'c.v.' stands for the central value obtained in the likelihood scan, and the expected central value is always unity, so it is not quoted explicitly.

Parameter	Condition	c.v.	Observed 68% | 95% CL		Expected 68% | 95% CL	
$\mu_F^{\text{off-shell}}$ ($2\ell2\nu + 4\ell$)	$\mu_V^{\text{off-shell}}$ unconst.	0.62	$[0.17, 1.3]$ | $[0.0060, 2.0]$		$[2 \cdot 10^{-5}, 2.1]$ | < 3.0	
$\mu_F^{\text{off-shell}}$ ($2\ell2\nu$)	$\mu_V^{\text{off-shell}}$ unconst.	0.41	$[0.014, 1.4]$ | < 2.6		< 2.5 | < 3.7	
$\mu_V^{\text{off-shell}}$ ($2\ell2\nu + 4\ell$)	$\mu_F^{\text{off-shell}}$ unconst.	0.90	$[0.31, 1.8]$ | $[0.051, 2.9]$		$[0.11, 3.0]$ | < 4.5	
$\mu_V^{\text{off-shell}}$ ($2\ell2\nu$)	$\mu_F^{\text{off-shell}}$ unconst.	1.1	$[0.28, 2.4]$ | $[0.016, 3.8]$		$[0.07, 3.2]$ | < 4.8	
$\mu^{\text{off-shell}}$ ($2\ell2\nu + 4\ell$)	$R_{V,F}^{\text{off-shell}} = 1$	0.74	$[0.36, 1.3]$ | $[0.13, 1.8]$		$[0.16, 2.0]$ | $[0.0086, 2.7]$	
	$R_{V,F}^{\text{off-shell}}$ unconst.	0.62	$[0.17, 1.3]$ | $[0.0061, 2.0]$		$[4 \cdot 10^{-5}, 2.1]$ | $[1 \cdot 10^{-5}, 3.0]$	
$\mu^{\text{off-shell}}$ ($2\ell2\nu$)	$R_{V,F}^{\text{off-shell}} = 1$	0.74	$[0.25, 1.5]$ | $[0.043, 2.3]$		$[0.11, 2.3]$ | $[2 \cdot 10^{-4}, 3.2]$	
	$R_{V,F}^{\text{off-shell}}$ unconst.	0.41	$[0.014, 1.4]$ | $[2 \cdot 10^{-5}, 2.6]$		$[3 \cdot 10^{-5}, 2.5]$ | $[6 \cdot 10^{-6}, 3.7]$	

Table 10: Summary of allowed 68% CL (central values with uncertainties) and 95% CL (in square brackets) intervals for $\mu^{\text{off-shell}}$, $\mu_{\text{F}}^{\text{off-shell}}$, and $\mu_{\text{V}}^{\text{off-shell}}$ obtained from the analysis of the combination of Run 1 and Run 2 off-shell data sets.

Parameter	Observed	Expected
$\mu^{\text{off-shell}}$	$0.78^{+0.72}_{-0.53}$ [0.02, 2.28]	$1.00^{+1.20}_{-0.99}$ [0.0, 3.2]
$\mu_{\text{F}}^{\text{off-shell}}$	$0.86^{+0.92}_{-0.68}$ [0.0, 2.7]	$1.0^{+1.3}_{-1.0}$ [0.0, 3.5]
$\mu_{\text{V}}^{\text{off-shell}}$	$0.67^{+1.26}_{-0.61}$ [0.0, 3.6]	$1.0^{+3.8}_{-1.0}$ [0.0, 8.4]

arXiv:1901.00174

Table 2: The 95% CL upper limits on $\mu_{\text{off-shell}}$, $\Gamma_H/\Gamma_H^{\text{SM}}$ and R_{gg}. Both the observed and expected limits are given. The 1σ (2σ) uncertainties represent 68% (95%) confidence intervals for the expected limit. The upper limits are evaluated using the CL_s method, with the SM values as the alternative hypothesis for each interpretation.

| | | Observed | Expected | | |
			Median	$\pm 1\,\sigma$	$\pm 2\,\sigma$
	$ZZ \rightarrow 4\ell$ analysis	4.5	4.3	[3.3, 5.4]	[2.7, 7.1]
$\mu_{\text{off-shell}}$	$ZZ \rightarrow 2\ell 2\nu$ analysis	5.3	4.4	[3.4, 5.5]	[2.8, 7.0]
	Combined	3.8	3.4	[2.7, 4.2]	[2.3, 5.3]
$\Gamma_H/\Gamma_H^{\text{SM}}$	Combined	3.5	3.7	[2.9, 4.8]	[2.4, 6.5]
R_{gg}	Combined	4.3	4.1	[3.3, 5.6]	[2.7, 8.2]

arXiv:1808.01191v2

Most of the systematics affect both the shape and normalization

- Theoretical uncertainties:
    - Renormalization scale and Factorization scale (up to 30%)
    - $\alpha_S(m_Z)$ and PDF variations (up to 20%)
    - Simulation of the second jet in gg samples (up to 20%)
    - Scale and tune variations of PYTHIA
    - NLO EW correction ($q\bar{q} \to ZZ, WZ$)
    - Uncorrelated uncertainties on $N_j = 0$ (2.7%), $N_j = 1$ (6.0%) and $N_j \geq 2$ (7.6%) in $q\bar{q} \to ZZ, WZ$ derived from the 3ℓ CR

- Instrumental uncertainties on the simulations:
    - Luminosity (between 1.2% and 2.5%, depending on the data taking period)
    - L1 prefiring scale
    - Pile-up, JES, JER and p_T^{miss} resolution correction
    - Uncertainties in lepton, trigger, pile-up jet identification, and b-tagging efficiencies (typically 1% per lepton)

Statistical uncertainties on simulations are also taken into account.